International Journal of Material Forming (2020) 13:1015–1024
https://doi.org/10.1007/s12289-019-01526-y

ORIGINAL RESEARCH

Investigation of various necking criteria for sheet metal formability analysis using digital image strain data

Yang Song[1] · Daniel E. Green[1] · Alexandra Rose[1]

Received: 30 January 2019 / Accepted: 17 November 2019 / Published online: 16 December 2019

Abstract

The precise determination of the forming limit strains of a sheet metal is necessary in order to accurately predict the onset of failure in sheet metal forming processes. The method used to detect the onset of necking (i.e. the necking criterion) is a most important factor in formability analysis as it significantly affects the forming limit strains. Many different necking criteria have been developed, which take advantage of the flexibility and high resolution of digital image correlation (DIC) strain measurements. Several time-dependent and time/geometry-dependent necking criteria were carefully investigated in order to evaluate their ability to reliably and consistently detect the onset of necking of TRIP780 sheet specimens that were stretch-formed over a hemispherical punch. It was found that the geometry-dependent, surface slope criterion was the most robust and consistent criterion of those evaluated.

Keywords Forming limit · Nakazima test · TRIP steel · DIC · Necking criterion

Introduction

Automotive and aerospace manufacturers use a wide range of sheet metal alloys to form parts with complex shapes and features. During a forming process, a metal sheet is stretched or drawn into shape between a pair of mating dies and the sheet safely deforms until it reaches its limit of formability. When the formability of the sheet metal is exhausted, the strains tend to localize in a narrow band and a through-thickness neck develops, thus compromising the structural integrity of the part.

Determining the forming limit of a particular sheet metal with accuracy is essential in order to reliably predict the outcome of a forming process. For several decades, forming limit curves (FLC) have been effectively used to assess the robustness of forming operations. An FLC is a curve that represents the lowest threshold strain states in a major strain versus minor strain coordinate system. This threshold is defined as the condition where the material is at risk of developing a neck. The sheet metal forming industry has adopted this model of representing the forming limit of a given sheet metal for numerical modeling and process design as it represents the strain state of maximum plastic deformation for the material based on experimental data. The Keeler method is traditionally used for the experimental determination of FLCs in North America [1]. It uses electro-etched grids to mark un-deformed specimens and requires that the forming process be stopped just at the onset of necking. The spatial resolution of the strains measured from electro-etched grids is generally 2.5 mm (0.1 in.). Moreover, the strains measured in a neck represent a single state of deformation that may, or may not, have occurred at the exact moment when necking started. Finally, the conventional grid analysis method does not take into account the strain history throughout the forming process prior to the start of necking.

The DIC is a non-contact surface deformation measurement method which replaces the Keeler method using digital images recorded throughout the deformation history of the sheet metal specimen. The DIC method uses a random, high-contrast pattern (referred to as a speckle pattern) which is applied to the sheet in the un-deformed state. The introduction and development of DIC has helped to reveal significantly more information in the process of forming sheet metal [2]. The DIC systems can easily reach sub-millimeter level spatial resolution for a standard size formability test specimen. The DIC method supplies a considerable quantity of data as it provides a high-resolution measure of the surface strain on the specimen at very fine time increments throughout the

✉ Yang Song
songw@uwindsor.ca

[1] Mechanical, Automotive and Materials Engineering, University of Windsor, Windsor, ON N9B 3P4, Canada

entire forming process. With the increased quantity and resolution of strain data collected from experiments using DIC, more details in the deformation history can be revealed to more accurately capture the forming limit of sheet metals. A number of necking criteria have been proposed which take advantage of the increase in spatial and time resolution of the strain data. This research aims to investigate the sensitivity and robustness of some of these necking criteria for detecting the onset of necking in a TRIP780 steel sheet stretched-formed over a hemispherical punch.

Overview of necking criteria

In the past decade, DIC has been extensively used in combination with different data analysis techniques to determine the onset of localized necking in formability specimens. Necking criteria can generally be classified into geometry-dependent and time-dependent criteria, although some criteria are based on both geometry and time. The main difference between the two approaches is whether the state variables being used to identify the onset of necking capture the unique geometrical profile of the specimen's top surface in at least two dimensions. For example, the vertical displacement of consecutive points on a three-dimensional (3D)-curve that lies across the specimen surface and their spatial derivatives are geometry-dependent state variables, and the history of these state variables is both time- and geometry-dependent. However, the evolution of the major strain or the strain rate at one point on the specimen is only time-dependent. Another way to distinguish between these two approaches is to examine whether changing the test rate would change the identification of the onset of necking. Necking criteria that are geometry-dependent are sometimes considered superior [3] to those that are only time-dependent, because localized necking is a macro-scale, through-thickness geometrical change.

The following sub-sections provide a review of some of the necking criteria that have been proposed by different researchers for identifying the onset of necking in sheet specimens.

The surface slope criterion

The surface slope criterion, proposed by Martinez-Donaire et al. [4], takes advantage of DIC data having a high resolution in both space and time. This is a time- and geometry-dependent criterion that detects the onset of necking using state variables derived from a 3D-curve that lies along the surface of the specimen, perpendicular to the neck that eventually develops during the test.

This criterion assumes the test specimen wraps around the hemispherical punch and its outer surface deforms into a geometry that very closely resembles that of the punch (with an offset corresponding to the sheet thickness, as it is affected by the through-thickness strain), as long as the thickness strain has not localized. The onset of necking is considered to occur at the moment when the top surface of the specimen ceases to resemble the shape of the punch.

This method computes the profile of a curve that lies across the neck on the outer surface of the specimen (i.e. height (z) vs. position (x)) throughout the time domain. The onset of necking occurs at the moment in time when this profile develops a flat region, that is, when the slope of the curve (derivative dz/dx) becomes constant. The position measurements obtained from the DIC must be passed through a robust frequency low-pass digital differentiator. And further measures may be required in order to overcome variability and imperfections in the data, such as the development of multiple necks.

The 3D-curvature criterion

The 3D-curvature method, proposed by Min et al. [5], is another time- and geometry-dependent criterion. This method uses state variables derived from several 3D curves that lie on the surface of the specimen and parallel to the neck that eventually develops. At the onset of necking, one or more dimples appear along the 3D-curve that lies in, and along, the neck, and the curvature of the fitted 3D-curve will change drastically when the dimples appear. In order to exaggerate the change in curvature, the 3D-curve can be converted from x-z displacements to an R-D coordinate system, where R is the radial distance to the center of the hemispherical punch and D is the arc-length from one end of the curve. And the onset of necking is identified at the start of the sudden change in curvature of the curve that lies in the neck.

The strain-rate criterion

A time-dependent necking criterion has been investigated by Zhang et al. [6] and Martinez-Donaire et al. [4], in which the onset of necking is identified by a change in major strain rate for two different points, one in the neck and one outside the neck-affected area. Since strain localization occurs in a narrow band in proximity to the final neck, the material outside this band will exhibit a gradual decrease in major strain rate. It is suggested that the onset of necking occurs when the strain rate of an "element" outside the necking area reaches its maximum. A frequency low-pass differentiator may be required to determine the strain rate from the DIC strain data.

The strain-acceleration criterion

Huang et al. [7] developed another time-dependent criterion, which searches for a sudden change in the major strain rate at a point in the neck. As a through-thickness neck initiates, the major strain will localize in the neck, and the major strain rate in the neck will increase at a faster rate. The onset of necking is identified when the second derivative of the major strain in the neck starts to deviate from a constant value.

The transition of incremental strain path criterion

The transition of strain path criterion is based on the theory that the strain path gradually changes to plane strain where the minor strain rate (in the direction parallel with the neck) decreases to zero at the onset of necking [8]. The width strain (ε_{22}) of an "element" inside the neck tends toward zero, while the major strain (ε_{11}) of an "element" outside the necking zone also tends toward zero (i.e. the incremental strain ratio $\Delta\varepsilon_{22}/\Delta\varepsilon_{11}$ outside the neck tends to minus infinity). This method is quite similar to the strain-rate criterion but shows a more exaggerated trend. It is also a time-dependent criterion because the state variable used to identify the onset of necking is only based on two locations on the specimen surface.

Bragard method

In 1972, Bragard [9] developed an approach for determining forming limit strains by taking the last frame before fracture or the first frame after fracture on a failed specimen. The strain state corresponding to the forming limit at the location of failure is calculated from an inverse parabola fitted from the major strain versus major displacement data. This method was adopted in the ISO12004-2 Standard for experimental determination of FLC [10]. One advantage of this method is that it allows the determination of the forming limit when the materials do not exhibit necking or barely exhibit necking before fracture, although the resulting FLC may be questionable as the forming limit strains are not experimentally measured. This method should be considered to be geometry-dependent and not time-dependent because it utilizes state variables along multiple 3D-curves across the neck to fit an inverse parabola to obtain the forming limit strains. It remains debatable if this method can really be considered a necking criterion due to the lack of definition of necking.

Material and experimental setup

Transformation-induced plasticity (TRIP) steels are a family of steel grades that belongs to the first generation of advanced high strength steels (AHSS), and they have been effectively used to form stronger and lighter automotive parts. TRIP steels have a microstructure that typically contains at least three, and often four, different phases: ferrite, bainite, retained austenite and martensite. The typical microstructure of TRIP steels contains at least 5% retained austenite [11]. The TRIP780 investigated in this study was supplied by ArcelorMittal Dofasco, and an Automotive Partnership Canada research project database provided the material data [12]. The chemical composition of the TRIP780 steel sheets is shown in Table 1, and the as-received mechanical properties are shown in Table 2.

Nakazima tests [13] were performed in a double-action hydraulic press, with LVDT position sensors to measure blankholder and punch travel, and load cells to measure blankholder and punch forces. A data acquisition system records the loads and positions at a frequency of 30 Hz. Dual Point Grey GRAS-50S5M-C cameras, each having a resolution of 5 MPx, were equipped with Schneider Xenoplan 35-mm lenses, connected in parallel and mounted with a 30° angle between the cameras, to ensure a complete and clear view of the gauge area of the specimen. Cameras are hardware triggered by NI USB 6221 DAQ and images are captured at a rate of 12 Hz. An LED Fresnel light is used to illuminate the specimen surface. The experimental setup is described in detail in previous work by Song [14].

Specimen geometries were designed to generate six different strain paths, with #1, #3 and #6 leading to uniaxial tension, plane-strain and balanced-biaxial tension, respectively. Specimen #1 has a gauge width of 12.5 mm, a gauge length of 25.4 mm and a transition radius of 30 mm. Specimens #2, #3 and #4 have a gauge width of 15 mm, 50 mm and 100 mm, respectively, measured at the minimum distance between the transition radius of 30 mm on each side of the specimen. Specimen #5 has two 20-mm-diameter holes that have a centre-to-centre distance between them of 160 mm. Finally, Specimen #6 is simply a 230-mm square blank. Figure 1 is a graph showing the typical strain paths determined at the necking location for each type of specimen, with illustrations of their corresponding geometries. A section view of the tooling for the Nakazima test is shown in Fig. 2.

Table 1 Chemical composition of 1.5 mm TRIP780 steel sheet

C	Mn	P	S	Si	Al	Cu	Ni
0.21	1.74	0.01	0.002	0.05	0.49	<.02	<.02
Cr	**Sn**	**Mo**	**V**	**Nb**	**Ti**	**B**	**N**
0.2	<.02	<.02	<0.008	0.015	0.003	0.0002	0.0022

Table 2 Material properties of 1.5 mm TRIP780 steel sheet

Grade	Yield (MPa)	Coating Type	Coating Weight
TRIP 780	462	Galvannealed	43 g/m2
UTS (MPa)	Unif. Elong. (%)	Total Elong. (%)	n (10–20%)
855	17.2	22	0.19

A random speckle pattern with consistent dot size was applied to each un-deformed Nakazima specimen by spraying a white mat paint on its surface as the base coat, and then spraying black paint with throttled nozzle, on top of the base coat. The friction between the punch and the sheet specimen was minimized by using a tribosystem of Vaseline® and PTFE film, placed between the punch and the specimen.

Correlated Solutions Vic-Snap 8, Vic-3D 2012 and a custom MATLAB code were used to capture and analyse stereo images for DIC output. The subset size of 35 pixels was selected to properly accommodate the dot size in the speckle pattern, and a step size of 5 pixels was used. The average projection error was kept below 0.07 pixel throughout all tests, and the noise in strain measurement is estimated to be 0.2% engineering strain, using rigid body motion tests. The one-standard deviation confidence interval for point match in each direction was observed to scale linearly with increasing strain, and could reach 0.02 pixel at around 40% strain. This leads to a ± 1% uncertainty in strain measurement for each tensorial strain component at a step size of 5 pixels.

Results and discussion

The DIC and press output for the Nakazima tests were processed with a MATLAB code designed to determine forming limit strains using different necking criteria in a practically fully automated process. A material *x*-*y*-*z* coordinate system was established, as shown in Fig. 3, and von Mises effective strains were calculated across the *x*-*y* grid on the outer surface

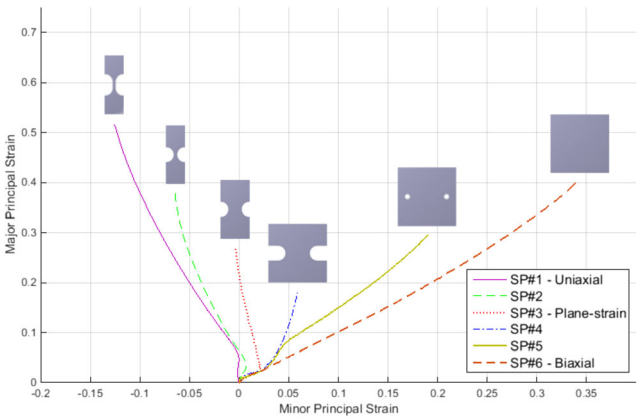

Fig. 1 Experimental strain paths in the Nakazima tests determined using DIC

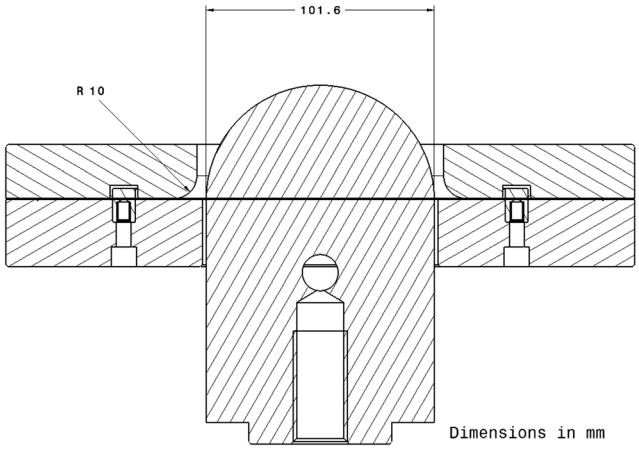

Fig. 2 Section view of Nakazima test tooling

of the specimen. The location of the maximum effective strain in the *x*-*y*-time domain was used to automatically identify the location of failure, that is, the location of the onset of necking which later becomes the fracture site. For each specimen analyzed, it was verified in the series of sequential digital images that the location of maximum effective strain in the *x*-*y* grid was indeed the location where necking started, and developed and where fracture eventually occurred. Fig. 4 shows an example of the effective strain distribution across a Nakazima specimen with the location of the maximum effective strain coinciding with the failure location from the onset of necking until a crack develops at this location. The forming limit strains were then calculated based on this identified failure location on the specimen when a time-dependent necking criterion was used.

Five necking criteria were implemented in the MATLAB code to analyse the DIC strain data: the surface slope criterion, the strain-rate criterion, the transition of incremental strain path criterion, the strain-acceleration criterion, and the 3D-curvature criterion. The transition of incremental strain path criterion did not provide consistent results, using the state

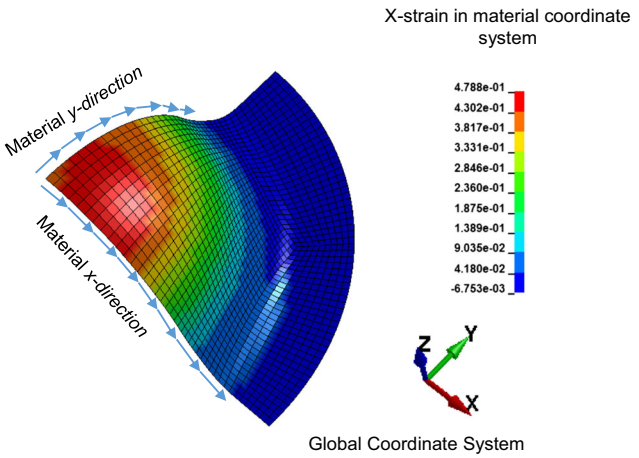

Fig. 3 Model of a quarter Nakazima specimen showing the material coordinate system

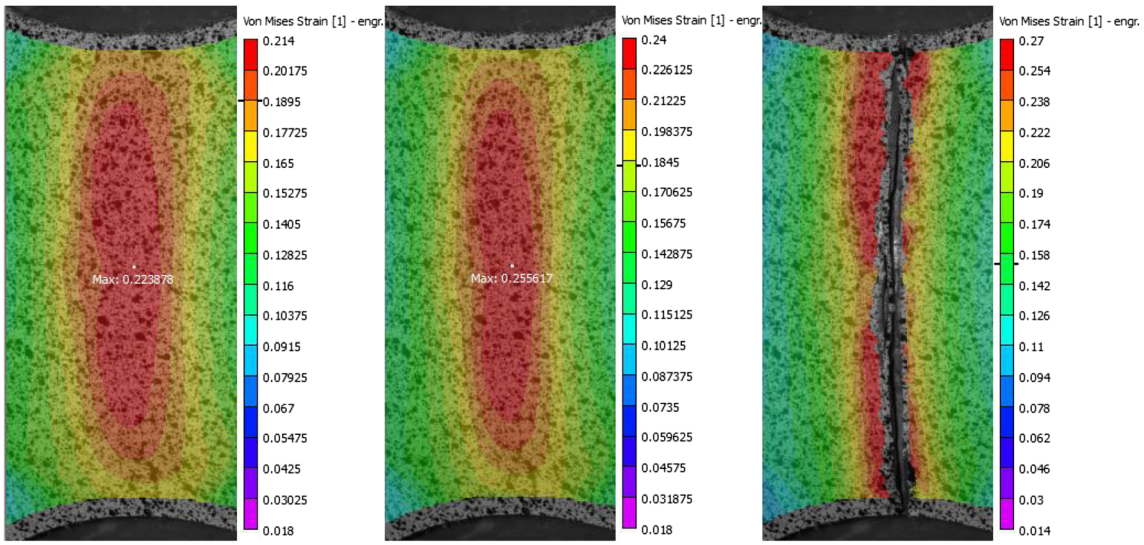

Fig. 4 Distribution of the effective strain across a Nakazima specimen (Specimen #3) showing that the failure location coincides with the location of maximum effective strain which remains unchanged from the onset of necking (left image) until the last image before fracture (middle image). The first image after fracture (right image) shows the fracture passing through this same location

variables specified in the literature ($\Delta\varepsilon_{22}/\Delta\varepsilon_{11}$), even though different threshold values and filtering parameters were evaluated. Therefore, these results are not included or discussed here.

Of the four remaining necking criteria, the surface slope criterion yields the least conservative forming limit strains. Figure 5 shows the forming limit diagram (FLD) obtained using this criterion, along with the forming limit strains obtained from each individual test specimen. The *x*-*z* coordinates of 11 curve sections lying across the neck were taken from the specimen surface profile, with a spacing of 0.25 mm between each curve, and the central curve, shown in Fig. 6a, is made to pass exactly through the "position of failure". The coordinate data for this central curve are then spatially differentiated twice, as shown in Fig. 6b and c. This analysis of the DIC data is repeated for each time-step and the maximum of the second derivative is tracked in time, as shown in Fig. 6d). The onset of necking is identified when the maximum value of the second derivative reaches zero. In the example shown in Fig. 6a-c, the neck initiates on the right side of the apex of the dome (at approximately $x = 60$ mm). And as shown in Fig. 6b, the first derivative dz/dx corresponding to the flat portion reaches a constant value. Finally, the onset of necking can be identified, regardless of its location on the specimen, when the maximum of the second spatial derivative reaches zero. This criterion has proven to be very robust and generally does not require much filtering for differentiation. Even when some minor filtering is applied, the identification of the onset of necking does not seem to be affected, because the differentiation is performed purely on spatial data, which does not affect the identification of onset of necking in time. Necking limit strains were calculated for each test specimen without requiring any subjective operator input.

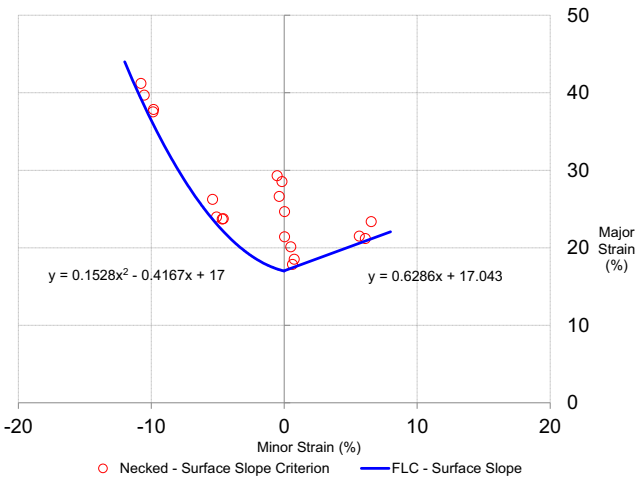

Fig. 5 FLD of TRIP780 determined using the surface slope criterion

For the specimens with geometries that lead to minor strains greater than +7% (Specimens #5 and #6), fracture was observed to occur suddenly without any evidence of necking. For these specimens, further analysis of these strain data is required and will be discussed in the paragraphs associated with Fig. 15.

The FLD obtained using the 3D-curvature criterion is shown in Figure 7. The *y*-*z* coordinates of 13 curve sections parallel to the neck were identified on the specimen surface, with a spacing of 0.25 mm, and the central curve passes exactly through the "position of failure" which was determined using a search for the maximum effective strain. Fig. 8a shows the configuration for selecting the curve sections. Again, the *y*-*z* coordinates were converted into *R*-*D* coordinates, with *R* being the distance to the center of the punch, and *D* being the arc-length from one end of the curve. An arc was fitted

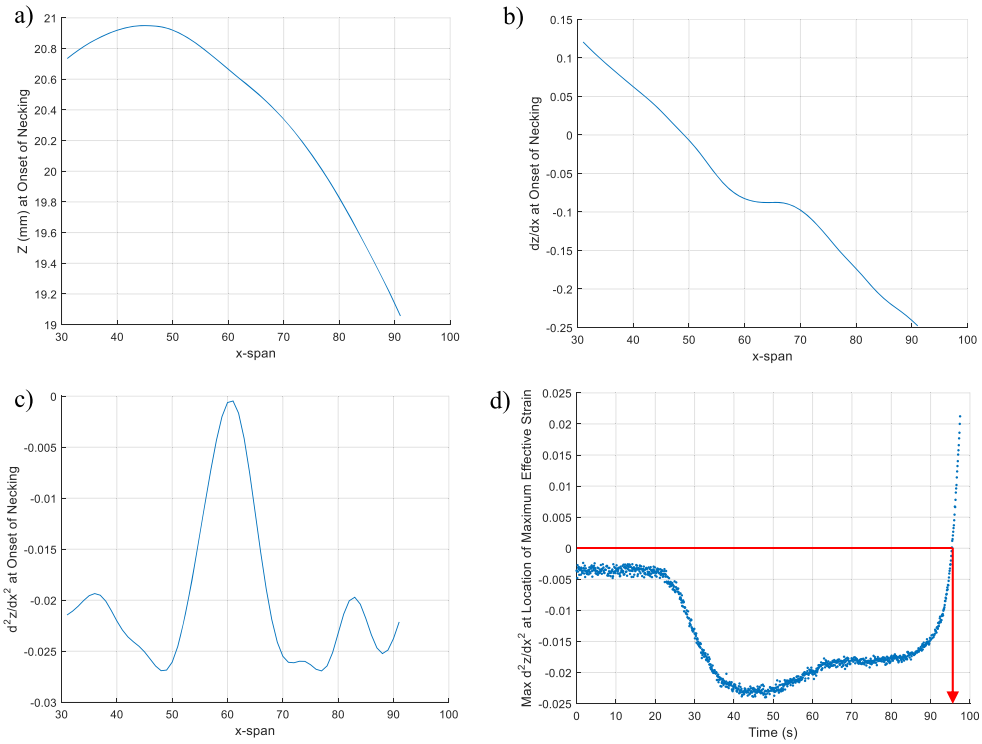

Fig. 6 Example of the analysis of state variables in the surface slope criterion – **a** Profile of the curve across the neck at onset of necking, **b** Spatial derivative of the curve across the neck at onset of necking, **c** Second spatial derivative of the curve across the neck at onset of necking, **d** Second spatial derivative history at necking location

to each processed curve and the local curvature was calculated, as shown in Fig. 8b. The onset of necking was identified with the sudden change in the curvature history, as marked by the red dot. Fig. 8c shows the x-y-R normalized surface height of the specimen (R, in millimeters), where evidence of grooves can be observed at the onset of necking. It is worth noting that for the strain paths approaching uniaxial tension, the 3D-curvature criterion shows a decreased sensitivity for detecting the onset of necking. The curvature history exhibits a more gradual change rather than a sudden increase, as shown in Fig. 8d. Since the change from diffused necking to localized necking is also more gradual for these strain paths, the exact location of necking is more ambiguous, and therefore it is more difficult to track curves that exactly overlap, or are parallel to, the neck. Another possible cause is that the specimens being used to generate these strain paths are so narrow that they do not fully wrap around the hemispherical punch in the minor direction, and moreover, the curves parallel to the neck are not sufficiently long to ensure a good fit. These factors lead to greater uncertainty. The authors who proposed this method also indicated that this criterion may present sensitivity issues when the curves for circle fitting are too short [5]. Nevertheless, in spite of the uncertainty introduced into the analysis of specimens whose strain path approaches uniaxial tension, the overall shape of the FLC does not change significantly. This method requires minimal operator input to ensure the quality of fit of the circles is adequate. Moreover, it is very sensitive for detecting the onset of localized necking.

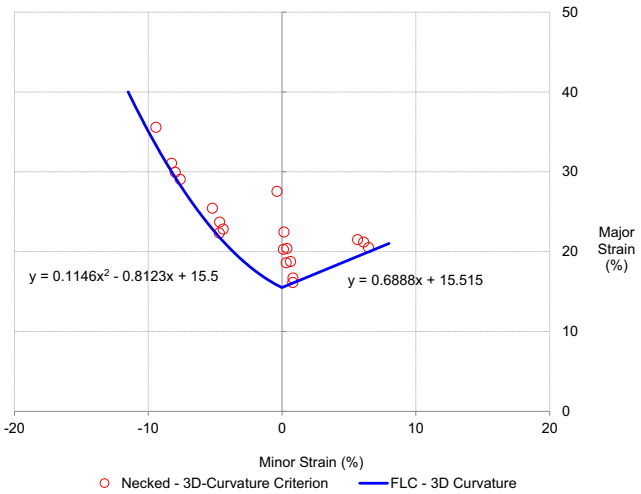

Fig. 7 FLD of TRIP780 determined using the 3D-curvature criterion

The FLD produced using the strain rate criterion is shown in Fig. 9. The strain rate criterion searches for the maximum major strain rate of a point that is "outside" the necking zone in the major strain direction. The distance from the centre of the neck to this outside point is commonly determined by multiplying the nominal thickness of the sheet by a factor of two. In the case of this TRIP780 sheet, which has a nominal thickness of 1.5 mm, it was verified that the point 3 mm away from the neck in the major strain direction is indeed outside the localized neck for all strain paths that produce a neck, as shown in the example in Fig. 10. Therefore, this factor of two was kept consistent for all the TRIP780 Nakazima specimens. However, this approach may require some subjective operator

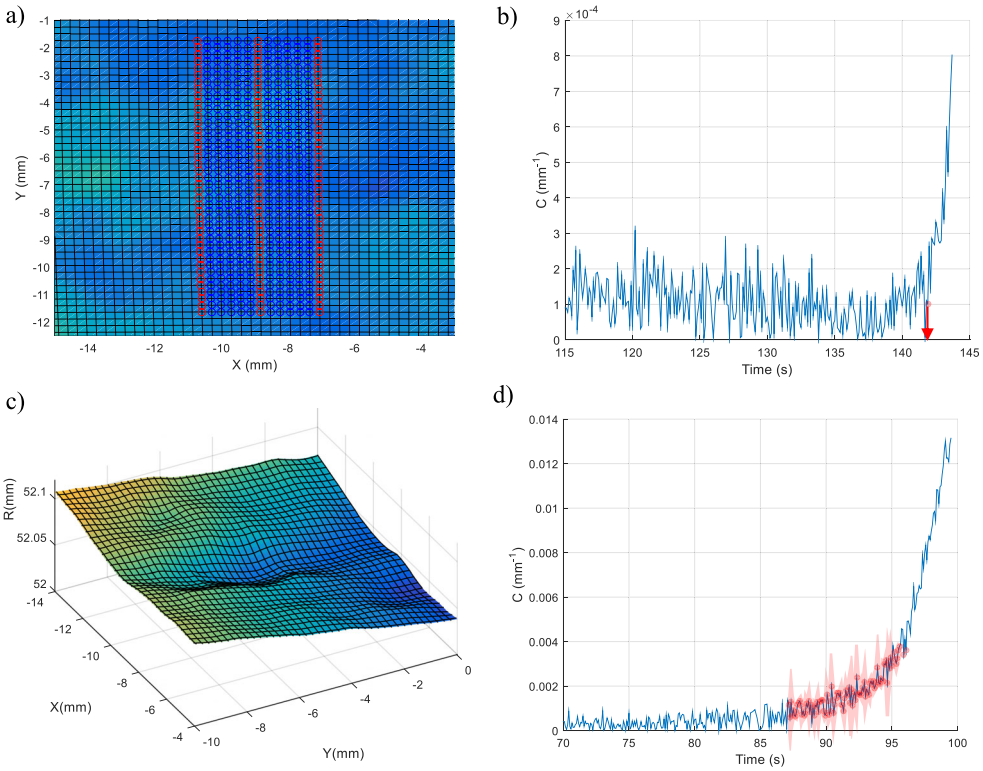

Fig. 8 Example of the analysis of state variables in the 3D-curvature criterion – **a** Effective strain distribution in the last frame with points for circle fit highlighted, **b** Circle fit curvature history, **c** *x*-*y*-R normalized surface profile (R) at onset of necking, **d** Circle fit curvature history showing decreased sensitivity to the onset of necking, compared to data in b).

input depending on the formability of the sheet material (e.g. a more ductile material may require a greater multiplier). A frequency low pass filtered digital differentiator [15] was used to calculate the strain rate due to the noise in the strain data. Since a phase lag is introduced by the use of any digital filter, the strain rates for the outside point was calculated twice, once in the chronological order, and once in reverse order, to compensate for the phase lag. As shown in Fig. 11, the time at the onset of necking is identified as the average of that of the peaks of the red (forward filtering) and the orange (reverse filtering) dashed curves. The strain-rate criterion only works when the specimen is formed to failure with a relatively stable test rate; a varying punch displacement rate, or an unusual change in the strain path will affect the determination of the onset of necking. Despite the sensitivity to strain rate variations, this method was found to be quite robust and can produce consistent forming limit strains without subjective input.

The strain acceleration criterion produces forming limit strains which differ slightly from those of the other three criteria, as shown in Fig. 12. Most of these variations are due to the method having lower sensitivity for detecting the onset of necking, as well as being prone to noise in the strain data and differentiation. According to Huang et al. [7], this

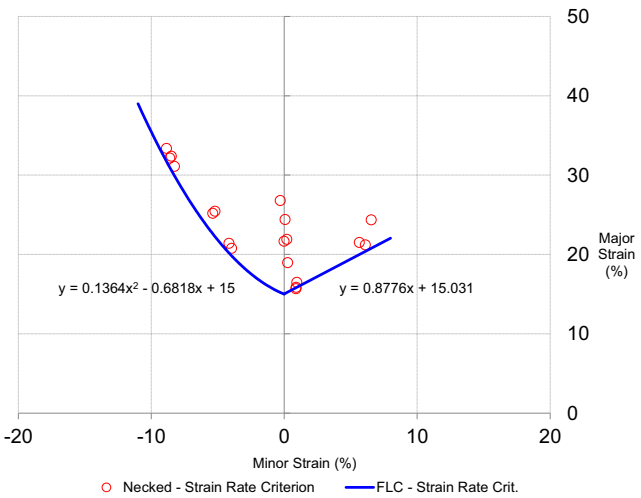

Fig. 9 FLD of TRIP780 determined using the strain-rate criterion

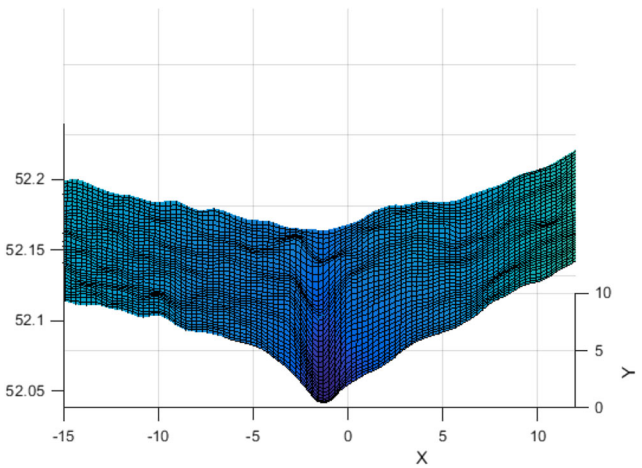

Fig. 10 DIC data showing the neck width at the last image before fracture

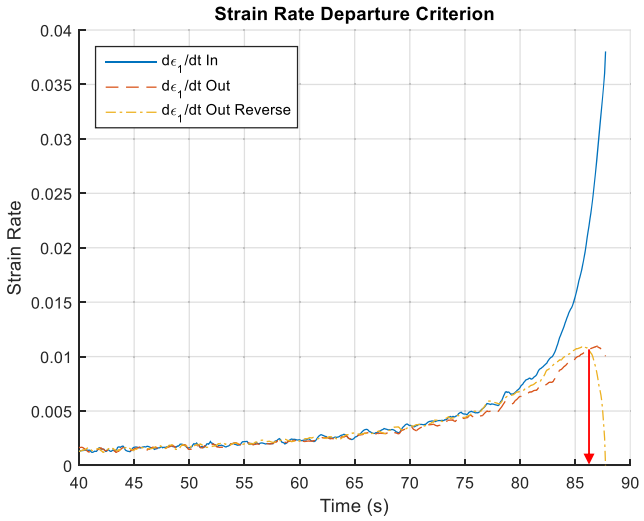

Fig. 11 Identification of the onset of necking using the strain-rate criterion

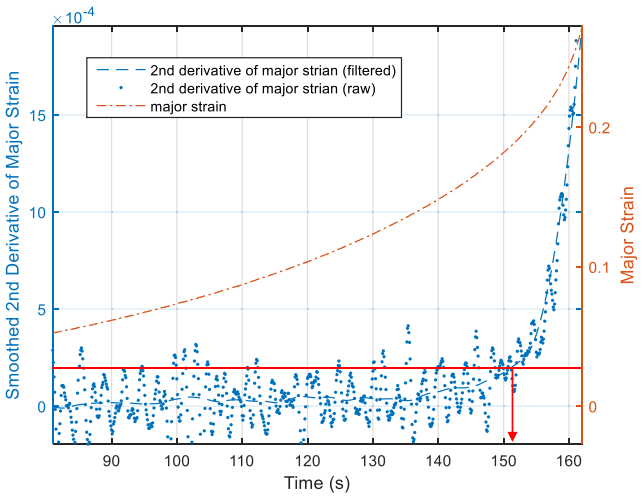

Fig. 13 Identification of the onset of necking using the strain-acceleration criterion

method identifies the onset of necking when the 2nd derivative of the major strain vs. time starts to deviate from a constant value. In reality, this change is generally a gradual increase instead of a sharp transition, therefore the sensitivity for detecting the onset of necking is relatively low. A threshold of 10% of the maximum value of the second derivative of the major strain was used to identify the onset of necking. Since strain differentiation inevitably amplifies high frequency noise, heavy filtering was required to help determine when the 2nd derivative exceeded this threshold. This filtering may also contribute to the decreased sensitivity for detecting the onset of necking. As shown in Fig. 13, the forming limit strains were determined with relatively greater uncertainty using the strain acceleration criterion.

Figure 14 shows a comparative plot of the four FLCs obtained by analysis of the DIC data. In addition, strain data obtained from square grid analysis (SGA) carried out on the same specimen geometries taken from the same sheet material and tested under the same conditions, are also shown in Fig. 14. The SGA process consists of first etching a 2.54 mm square grid onto flat, un-deformed sheet specimens, and then forming these in the Nakazima tool until a shallow neck becomes detectable by visual observation under incident lighting; this approach is consistent with press shop practice. The major and minor strains were then measured in grids that lie across the shallow localized neck using a calibrated grid analyzer from FMTI Systems Inc., and are identified in Fig. 14 as "necked SGA" data. It appears that the SGA data generally overestimate the forming limit, while the necking strains calculated from DIC data and the corresponding FLCs are more accurate. This is because the necking criteria based on DIC data identify the very onset of plastic instability, whereas SGA data are strain measurements made in locations that have been deformed somewhat beyond the onset of necking.

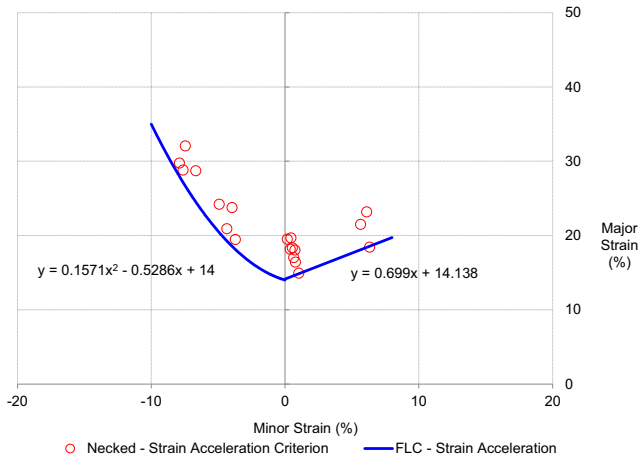

Fig. 12 FLD of TRIP780 determined using the strain acceleration criterion

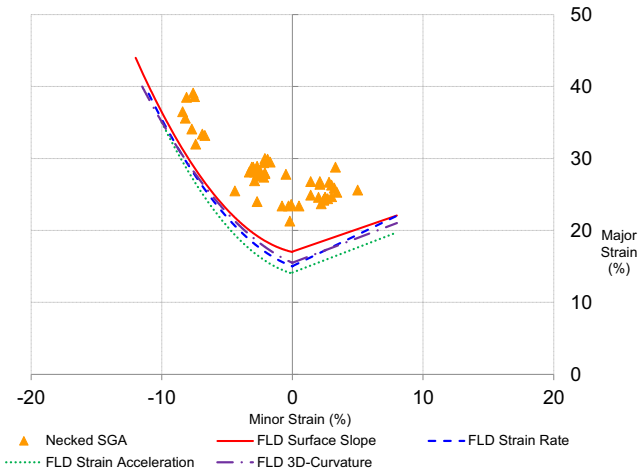

Fig. 14 Comparison of FLCs obtained using different necking criteria for DIC strain data with necked strain data obtained by conventional square grid analysis (SGA)

It can also be observed that the FLCs determined using the different necking criteria vary significantly for strain paths in the vicinity of plane strain, but the FLCs tend to converge for strain paths that approach uniaxial tension. This is perhaps because the left-hand-side of the FLC (negative minor strains) is typically observed to follow a line of constant thickness strain.

As mentioned previously, the Nakazima specimens with geometries that lead to strain paths in biaxial tension (Specimens #5 and #6) do not exhibit necking before cracking, and therefore the FLC is not available for minor strains that exceed +7%. Nevertheless, in order to estimate the limiting strains of this TRIP780 steel in biaxial tension, the DIC strain data obtained from these specimens were analysed according to the ISO 12004-2:2008 standard [10]. This method uses an inverse parabola fit of the major strain data obtained in the last frame before fracture and that lie along a line perpendicular to the location where fracture will occur. The limiting strain data obtained with the ISO method are shown in Fig. 15 as solid pink squares, and a pink dashed line shows the trend line of the ISO forming limit for minor strains in the range of +15% to +40%.

The maximum safe strains measured by DIC in the last image before fracture in Specimens #5 and #6 are also plotted in Fig. 15, and are shown as solid green circles. However, while the maximum safe strains and the ISO limiting strains might be useful as a lower-bound estimate of the limiting strains, they cannot be considered a part of the FLC of this sheet material because they are obtained from a digital image that does not show any evidence of necking. Since the strain paths in biaxial tension (i.e. for minor strains greater than +15%) lead to fracture without any prior necking, the forming limit of this material in this region of the strain diagram is actually a fracture forming limit (FFL). Various approaches have been proposed to determine the FFL of sheet materials, such as for instance the recent work of Borrego et al. [16]. However, the current experimental data shows that some specimens tested in biaxial tension followed a significantly non-linear strain path (see Fig. 1) and therefore further experimental work as well as rigorous data analysis will be required to accurately determine the FFL of this sheet material.

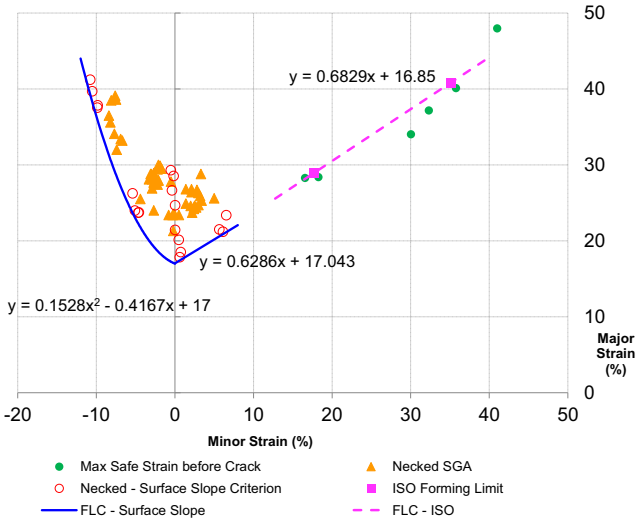

Fig. 15 FLD of TRIP780 determined using the surface slope criterion; in addition, strain data obtained using the ISO 12004-2:2008 standard as well as the maximum safe strains are shown in the region of biaxial tension, both measured from the last digital image before fracture

Conclusions

The FLC of 1.5 mm TRIP780 steel sheets was determined using four different necking criteria to analyse DIC strain measurements obtained during Nakazima tests. All four necking criteria were shown to be more accurate than the conventional SGA method in determining the onset of necking for this sheet material. The surface slope criterion was found to be the most robust and consistent criterion overall and is applicable over a wide range of strain paths. The 3D-curvature criterion has the greatest sensitivity for detecting the onset of necking, provided the specimen is sufficiently wide to accommodate the required curve lengths for circle fitting. Of the two time-dependent criteria, the strain rate criterion was the more consistent, when a reasonable neck width and a proper low-pass filter for strain differentiation is configured. More generally, time- and geometry-dependent necking criteria were observed to be more robust and more reliable than those that are only time-dependent. They require less input from the operator, and have greater sensitivity for detecting the onset of necking. It still remains to investigate the robustness of these necking criteria as they are used for the formability analysis of a variety of other sheet materials.

It was also observed that, when this TRIP780 steel is deformed in biaxial tension, sheet specimens suddenly fracture without any evidence of prior necking. Therefore, further rigorous work is required in order to accurately determine the FFL of this sheet material.

Acknowledgements ArcelorMittal Dofasco is gratefully acknowledged for providing the TRIP780 sheet steel along with the chemical composition and basic mechanical properties.

Conflict of interest The authors declare that they have no conflict of interest

References

1. Keeler S, Backofen WA (1963) Plastic instability and fracture in sheets stretched over rigid punches. Asm Trans Q 56(1):25–48
2. Min J, Stoughton TB, Carsley JE, Lin J (2017) Comparison of DIC methods of determining forming limit strains. Procedia Manuf 7: 668–674

3. Min J, Stoughton TB, Carsley JE, Lin J (2017) A method of detecting the onset of localized necking based on surface geometry measurements. Exp Mech 57(4):521–535
4. Martinez-Donaire AJ, Garcia-Lomas FJ, Vallellano C (2014) New approaches to detect the onset of localised necking in sheets under through-thickness strain gradients. Mater Des 57:135–145
5. Min J. Stoughton, TB, Carsley, JE and Lin, J (2017) An improved curvature method of detecting the onset of localized necking in Marciniak tests and its extension to Nakazima tests, Int J Mech Sci, vol. 123, no. January, pp. 238–252
6. Zhang C, Leotoing L, Zhao G, Guines D, Ragneau E (2011) A comparative study of different necking criteria for numerical and experimental prediction of FLCs. J Mater Eng Perform 20(6):1036–1042
7. G. Huang, S. Sriram, and B. Yan, "Digital image correlation technique and its application in forming limit curve determination," in Proceedings of the IDDRG 2008 International Conference, International Deep Drawing Research Group, June, 2008, pp. 16–18
8. Zhang C, Leotoing L, Guines D, Ragneau E (2009) Theoretical and numerical study of strain rate influence on AA5083 formability. J Mater Process Technol 209(8):3849–3858
9. Bragard, A, Baret, JC and Bonnarens, H Simplified Technique to Determine the FLD on the Onset of Necking, C. R. M., no. 33, pp. 53–63, 1972
10. International Organization for Standardization, "Metallic materials — Sheet and strip — Determination of forming-limit curves — Part 2: Determination of forming-limit curves in the laboratory," vol. 12004–2. International Organization for Standardization, Geneva, Switzerland, 2008
11. Tamarelli, CM, AHSS 101 the evolving use of advance high-strength steel for automotive applications, Southfield, 2011
12. Green D, Samei J, Hasannejadasl A, Jenab A, and Sari Sarraf I, Metal Forming Processes Research - APC Project (EHF), 2012. [Online]. Available: https://web2.uwindsor.ca/apc-ehf/index.html. Accessed: 25 Jul 2015
13. Nakazima K, Kikuma T, and Hasuka K, Study on the formability of steel sheets, Yawata Tech Rep, Sept., no. 264, pp. 8517–8530, 1968
14. Song Y, Investigation of the formability of TRIP780 steel sheets, MASc Thesis, University of Windsor, Canada, 2017
15. Luo J, Smooth Differentiation - File Exchange - MATLAB Central, 2004. [Online]. Available: https://www.mathworks.com/matlabcentral/fileexchange/6170-smooth-differentiation. Accessed 26 Sep 2016
16. Borrego M, Morales-Palma D, Martínez-Donaire AJ, Centeno G, Vallellano C (2019) Analysis of formability in conventional hole flanging of AA7075-O sheets: punch edge radius effect and limitations of the FLC. Int J Mater Form:1–14